



Swansea University
Prifysgol Abertawe



Cronfa - Swansea University Open Access Repository

This is an author produced version of a paper published in:

Nature Geoscience

Cronfa URL for this paper:

<http://cronfa.swan.ac.uk/Record/cronfa50792>

Paper:

Jones, M., Santín, C., van der Werf, G. & Doerr, S. (2019). Global fire emissions buffered by the production of pyrogenic carbon. *Nature Geoscience*

<http://dx.doi.org/10.1038/s41561-019-0403-x>

This item is brought to you by Swansea University. Any person downloading material is agreeing to abide by the terms of the repository licence. Copies of full text items may be used or reproduced in any format or medium, without prior permission for personal research or study, educational or non-commercial purposes only. The copyright for any work remains with the original author unless otherwise specified. The full-text must not be sold in any format or medium without the formal permission of the copyright holder.

Permission for multiple reproductions should be obtained from the original author.

Authors are personally responsible for adhering to copyright and publisher restrictions when uploading content to the repository.

<http://www.swansea.ac.uk/library/researchsupport/ris-support/>

Global fire emissions buffered by the production of recalcitrant pyrogenic carbon

Authors:

Matthew W. Jones^{1*}, Cristina Santín^{1,2}, Guido R. van der Werf³ and Stefan H. Doerr¹

Affiliations:

¹Geography Department, College of Science, Swansea University, Swansea, UK

²Biosciences Department, College of Science, Swansea University, Swansea, UK

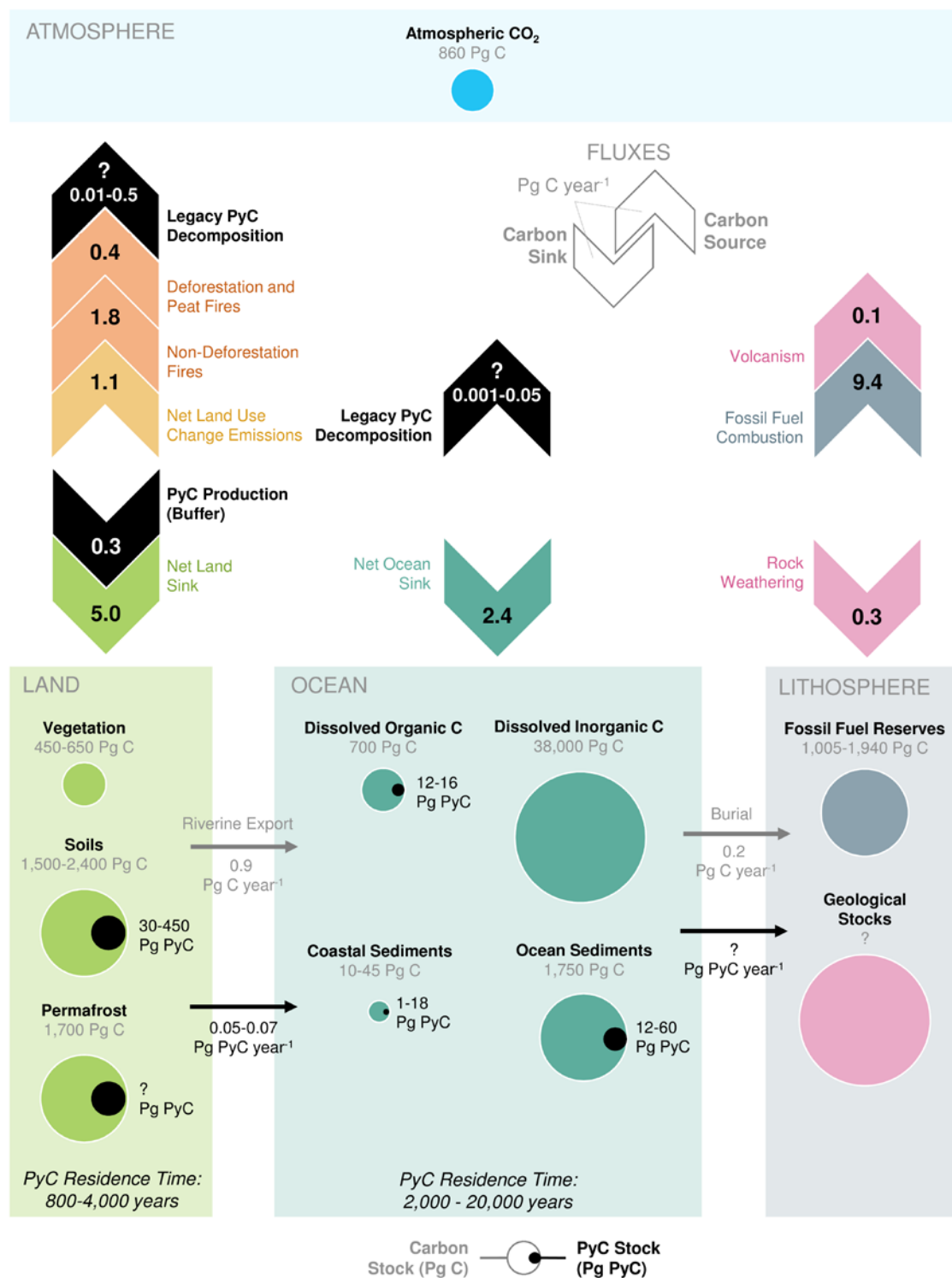
³Faculty of Science, Vrije Universiteit, Amsterdam, Netherlands

*e-mail: matthew.w.jones@swansea.ac.uk.

Landscape fires burn an estimated 3-5 million km² of the Earth's surface annually, emitting 2.2 Pg C year⁻¹ to the atmosphere while also converting a significant fraction of the carbon in burnt biomass to pyrogenic carbon (PyC) contained in combustion by-products. PyC can be stored in terrestrial and marine pools for centuries to millennia, buffering short-term emissions of carbon to the atmosphere by persisting as a recalcitrant pool of carbon during and following vegetation recovery. PyC stocks are routinely ignored in global models of the carbon cycle, leading to systematic errors in carbon accounting. Here we present a comprehensive new dataset of PyC production factors and merge this with the Global Fire Emissions Database (GFED4s+PyC) to quantify the global PyC production flux. GFED4s+PyC suggests that 256 (196-340) Tg C year⁻¹ was converted to PyC by biomass burning in the period 1997-2016, 91% of which occurred in the (sub)tropics. While savannah fires were consistently the largest source of PyC (49% on average), variation in tropical forest burning, driven by the El Niño Southern Oscillation, was the dominant driver of inter-annual variability in global PyC production. Our global estimate equates to 12% of the carbon emitted annually by landscape fires, indicating that the fate of a substantial fraction of the vegetation carbon stocks affected annually by fire is misrepresented in fire-enabled global models. We estimate that the cumulative production of PyC since 1750 (60 Pg C) is equivalent to ~33-40% of the global losses of biomass carbon due to land use change in the same period. Our results show that PyC production creates capacity for a quantitatively significant sink for atmospheric CO₂ that is presently missing from global carbon budget assessments.

32 Globally, landscape fires including wildfires, deforestation fires, and agricultural burns
33 emit approximately 2.2 Pg C year⁻¹ to the atmosphere (1997-2016)¹. This emission flux
34 includes ~0.4 Pg C year⁻¹ due to tropical deforestation and peatland fires, which contribute to
35 net global emissions of carbon due to land use change (~1.1-1.5 Pg C year⁻¹; Figure 1)²⁻⁴.
36 The emission fluxes resulting from biomass fires and land use change are outweighed by the
37 re-sequestration flux of carbon to undisturbed and re-growing vegetation (~5.0 Pg C year⁻¹;
38 Figure 1)⁵⁻⁸. These global carbon budget estimates are generated by models that represent
39 the temporally distinct processes of immediate carbon emission from burned areas and
40 decadal-scale re-sequestration through vegetation (re-)growth in a spatially explicit
41 manner^{1,9,10}. However, such models routinely overlook the coincident flux of biomass carbon
42 to recalcitrant by-products of fire, which can be stored in terrestrial and marine pools for
43 centuries to millennia, and thus provide a long-term buffer against fire emissions (Figure
44 1)^{7,11-14}. Consequently, the legacy effects of fire that operate on the longest timescales are
45 systematically excluded from models of the carbon cycle and from global carbon budgets^{13,15}.

46 These legacy effects are due to the incomplete combustion of vegetation during
47 landscape fires, which transforms organic carbon (OC) in biomass to a continuum of
48 thermally-altered products that are collectively termed pyrogenic carbon (PyC)^{11,13,16}. The
49 majority of the PyC produced during vegetation fires remains initially on the ground in
50 charcoal particles of varying size and is subsequently transferred to its major global stores in
51 soils¹⁷⁻¹⁹, sediments^{20,21} and ocean waters^{22,23}. A smaller fraction of fire-affected vegetation
52 carbon is emitted as PyC in smoke and has been studied extensively for its influence on
53 Earth's atmospheric and cryospheric radiative balances^{24,25}. PyC includes labile products of
54 depolymerisation reactions as well as aromatic molecules that result from condensation
55 reactions, the latter of which are depleted in functional groups and thus chemically and
56 biologically recalcitrant²⁶⁻²⁸. The enhanced resistance of PyC to biotic and abiotic
57 decomposition leads to its preferential storage in terrestrial and marine pools^{16,21} and a
58 residence time that is typically one to three orders of magnitude greater than that of its
59 unburnt precursors¹³. This makes PyC one of the largest groups of chemically discernible
60 compounds in soil with a contribution to soil organic carbon (SOC) stocks of 14% globally¹⁷.
61 PyC is also conserved across the land-to-ocean aquatic continuum and thus contributes
62 approximately 10% of riverine dissolved organic carbon²⁹, 16% of riverine particulate organic
63 carbon³⁰, and 20-50% of the organic carbon in ocean sediments¹⁴.



64

65 **Figure 1:** A simplified schematic of the global carbon cycle including the buffer and legacy roles of PyC. Stock
 66 values are expressed in Pg C (1 Pg C = 1 × 10¹⁵ g of carbon) and flux values are expressed in Pg C year⁻¹. The
 67 global carbon cycle is represented by values from the Global Carbon Budget assessment of the decade 2008–
 68 2017 (ref. ²) including: stocks of carbon in vegetation, soil, permafrost, ocean dissolved organic and inorganic
 69 matter, coastal and oceanic sediments, and fossil fuel reserves; fluxes of carbon due to the net land sink

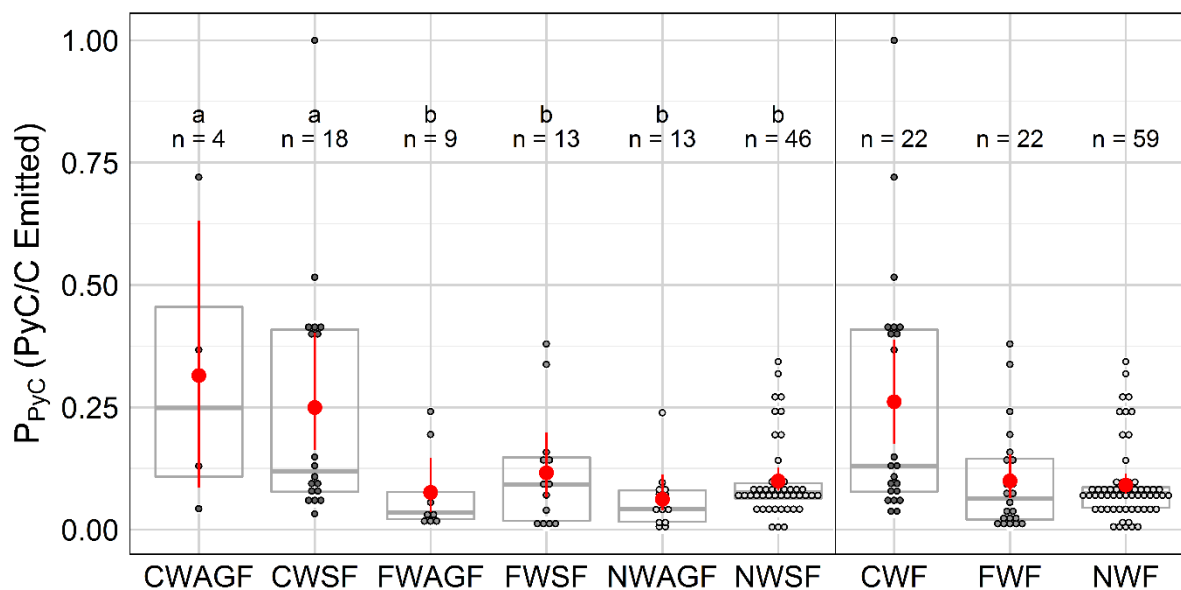
70 (modified to exclude non-deforestation fire emissions), fossil fuel combustion, the net ocean sink, and net land
71 use change emissions (modified to exclude deforestation fire emissions). Emission estimates from deforestation
72 and peat fires, and from non-deforestation fires derive from GFED4s and relate to the period 1997-2016 (ref. 1;
73 deforestation fires are restricted to the tropics). Carbon fluxes due to volcanism and rock weathering derive from
74 the IPCC AR5 assessment and relate to the period 2000-2009 (ref. 4). Pyrogenic carbon production fluxes due
75 to deforestation and non-deforestation fires are based on estimates from GFED4s+PyC and relate to the period
76 1997-2016 (this study). PyC stocks in soils, oceanic DOC and ocean sediments are based on representative
77 PyC/OC ratios from references 17, 31, and 14 applied to the Global Carbon Budget 2018 estimates of OC stocks
78 and fluxes. PyC fluxes through rivers are the sum of global dissolved and particulate PyC export fluxes from
79 references 29 and 30. Residence times shown for soils derive from references 32 and 26. Residence times for
80 oceanic PyC pools derive from references 20 and 33. Maximum (and minimum) legacy PyC decomposition fluxes
81 for land and ocean stocks are calculated as the product of high-end (and low-end) total stock magnitudes in
82 each domain and the reciprocal of the low-end (and high-end) estimate for residence time.

83
84 A series of reviews and data syntheses have recognised the potential of PyC
85 production to invoke a drawdown (sink) of photosynthetically-sequestered CO₂ to pools that
86 are stable on timescales relevant to anthropogenic climate change and its
87 mitigation^{7,11,13,14,34–37}. Owing to the relative recalcitrance of PyC, the conversion of biomass
88 carbon to PyC represents an extraction of carbon from a pool cycling on decadal timescales
89 to a pool cycling on centennial or millennial timescales^{14,20,21,26,38}. This storage potential
90 contrasts with that of dead vegetation, which otherwise contributes to post-fire emissions on
91 annual to decadal timescales or enters soil pools with a shorter residence time than that of
92 PyC^{9,12,26,39,40}. Consequently, post-fire PyC pools emit carbon to the atmosphere over a
93 significantly longer time period than would be the case in the absence of PyC production,
94 meanwhile providing a buffer that moderates atmospheric CO₂ stocks (Figure 1)^{7,13,14}. At
95 present, the fire-enabled vegetation models that are used to make global carbon budget
96 calculations account for short-term fire emissions but routinely exclude fluxes of carbon from
97 biomass to PyC or the delayed emission of carbon from legacy PyC stocks to the atmosphere
98 (Figure 1)^{9,10,15,41,42}. This introduces systematic errors to global carbon budgets through
99 misrepresentation of modern and historical fire effects on the net exchange of carbon
100 between the atmospheric and terrestrial-marine pools^{13–15}.

101 While PyC has been recognised as a major component of post-fire carbon stocks for
102 a number of decades^{11,37}, quantification of its production rate at the global scale has been
103 problematic and estimates vary by roughly an order of magnitude (50-379 Tg C year⁻¹)^{13,14,36}.

104 A cause of the large range of production estimates is that calculations have previously relied
 105 on incomplete information regarding the spatial distribution and type of fires, the allocation of
 106 carbon amongst biomass fuel components in burned areas and the specific PyC production
 107 factors for these distinct biomass fuel components. To alleviate these issues, we enhanced
 108 the Global Fire Emissions Database version 4 with small fires (GFED4s)¹, which is one of the
 109 principal process-based models used to make estimates of carbon emission from open
 110 biomass burning^{41,43,44}. Specifically, PyC production was incorporated by following a three-
 111 step approach consisting of: (i) the assembly of the most comprehensive global database of
 112 PyC production factors (P_{PyC} ; g PyC g⁻¹ C emitted) compiled to date; (ii) the assignment of
 113 production factors for individual fuel classes stratified as coarse or fine and as woody or non-
 114 woody (Figure 2), and; (iii) the application of production factor (P_{PyC}) values to fuel-stratified
 115 carbon emissions (CE; g C emitted) modelled by the native fuel consumption model in
 116 GFED4s. The output is the first global gridded dataset for monthly PyC production at a
 117 resolution of 0.25° × 0.25°, covering the years 1997-2016.

118



119

120 **Figure 1:** Box plots showing the distributions of PyC production factor (P_{PyC}) values for each of the biomass
 121 component classes in the production factor dataset. Abbreviations are: CWAGF, coarse woody aboveground
 122 fuels; CWSF, coarse woody surface fuels; FWAGF, fine woody aboveground fuels; FWSF, fine woody surface
 123 fuels; NWAGF, non-woody aboveground fuels; NWSF, non-woody surface fuels; CWF, coarse woody fuels
 124 (includes both CWSF and CWAGF); FWF, fine woody fuels (includes both FWAGF and FWSF); NWF, non-
 125 woody fuels (includes both NWAGF and NWSF). Dots mark the distribution of P_{PyC} values across 1% intervals

126 on the y-axis. Red dots show mean P_{PyC} values while red lines show the bootstrapped 95% confidence interval
127 (see methods). Boxes illustrate the median and interquartile range of values. Letters a and b indicate biomass
128 components with statistically similar P_{PyC} distributions at the 95% confidence level according to Tukey HSD
129 tests. The number of data entries (n) is also shown.

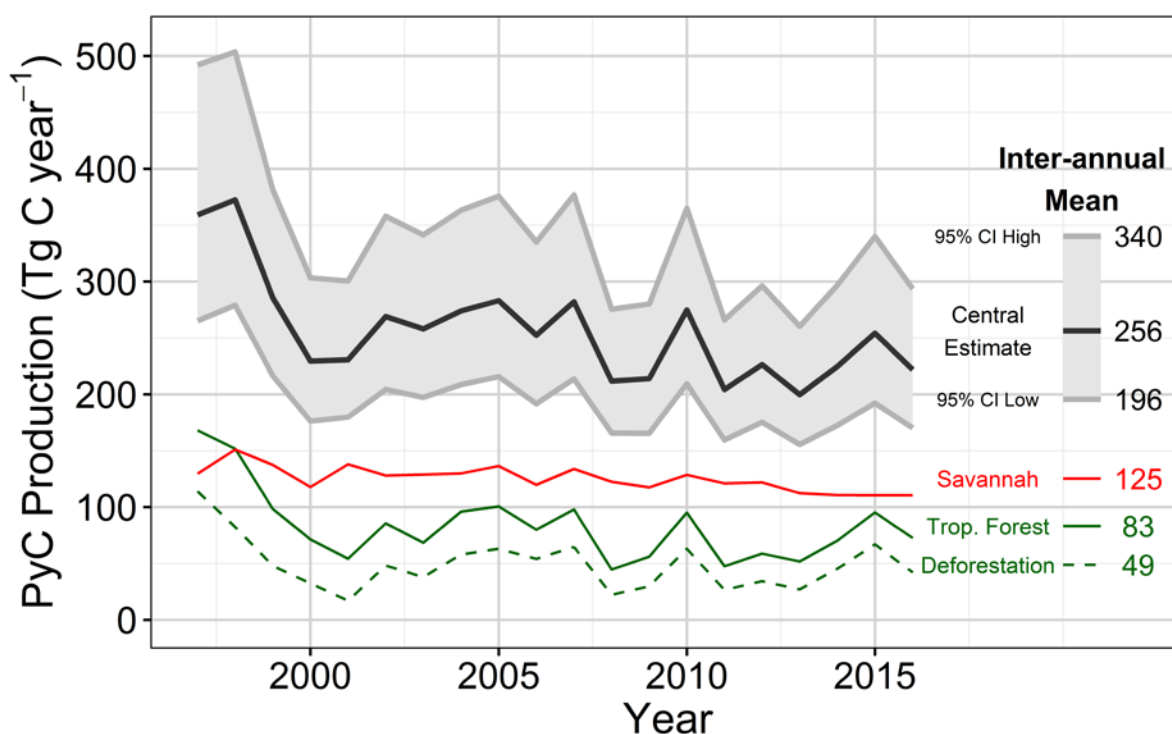
130

131 **Global PyC Production**

132 Our central estimate for global PyC production in the period 1997-2016 was 256 Tg C
133 year⁻¹ with an uncertainty range based on production factors of 196-340 Tg C year⁻¹ (Figure
134 3). Inter-annual variability in global PyC production, expressed as the standard deviation
135 around the mean, was 47 Tg C year⁻¹ and was most strongly associated with variability in
136 woody fuel combustion, including standing wood and coarse woody debris (CWD;
137 supplementary information text S1 and Figure S1). Coarse woody fuels produce PyC at a
138 greater rate than finer fuels (Figure 2) and consequently forest fires have disproportionate
139 potential to influence global rates of PyC production (supplementary Figure S2).

140 The El Niño Southern Oscillation (ENSO) is the primary driver of inter-annual variability
141 in burned area in the tropics⁴⁵ and previous analyses conducted with GFED have shown that
142 carbon emissions from tropical forest ecosystems more than doubled on average during
143 positive (El Niño) phases relative to negative (La Niña) ENSO phases⁴⁶. Correspondingly, we
144 calculated that global rates of PyC production in tropical forests were 111% greater during
145 the main fire season of El Niño phases than La Niña phases (supplementary Table S1). As
146 rates of PyC production by non-forest fires did not show a significant response to ENSO at
147 the global scale (supplementary Table S1), the response of forest fires was the major driver
148 of inter-annual variability in total PyC production (Figure 3). The production of PyC was
149 anomalously high in 1997-1998 (366 Tg C year⁻¹), aligning with a particularly strong positive
150 El Niño phase which promoted extensive burning of (tropical) forests in South and Central
151 America and in Southeast and Equatorial Asia^{1,46}.

152



153

154 **Figure 3:** Annual global PyC production estimates from GFED4s+PyC. The black line plots the modelled rate
 155 of production based on central P_{PyC} ratios ($g\ PyC\ g^{-1}\ C\ emitted$) from the global dataset. The shaded area
 156 indicates the uncertainty range of modelled values based on the 95% confidence intervals of P_{PyC} values (see
 157 Figure 2). The contributions of savannah burning and tropical forest burning to global production totals are
 158 shown, the latter of which includes deforestation fires (also shown; dashed line).

159

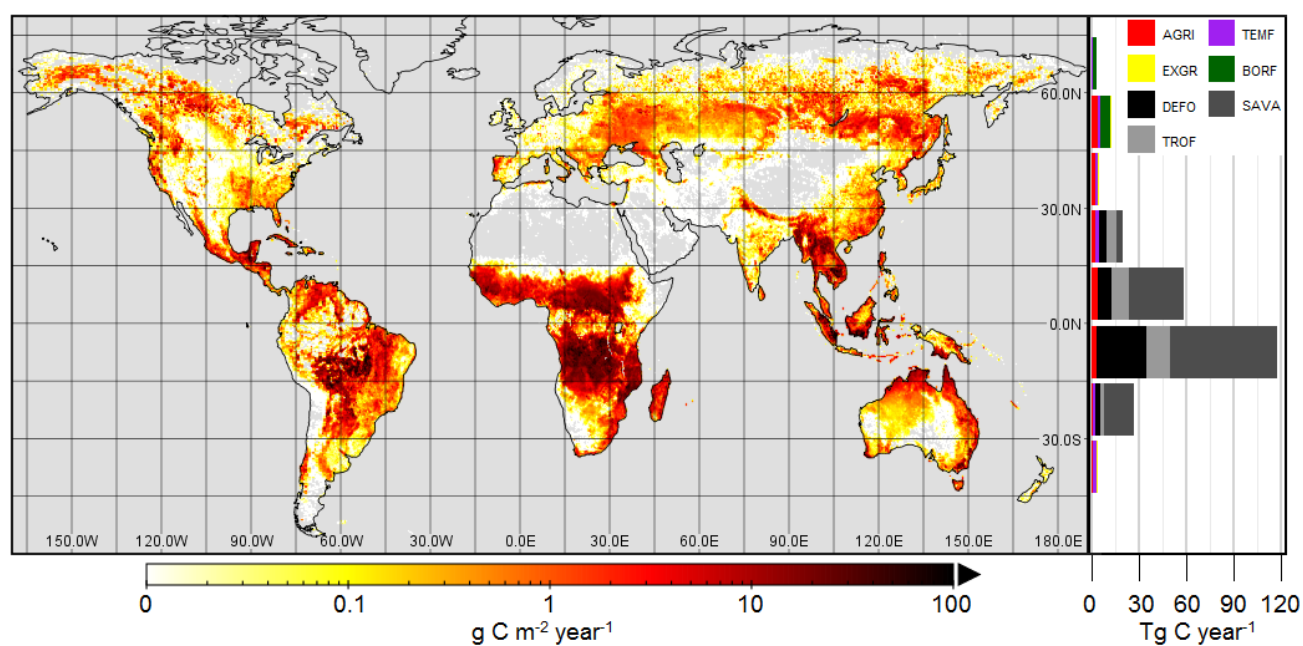
160 Major Production Regions

161 The PyC production rates modelled by GFED4s+PyC conformed to a latitudinal
 162 pattern (Figure 4), with the tropical latitudes clearly dominating production at the global scale.
 163 91% of global production occurred in the tropics and subtropics ($0-30^{\circ}\ N/S$), while temperate
 164 ($30-60^{\circ}\ N/S$) and high-latitude regions ($60-90^{\circ}\ N$) provided small contributions to the global
 165 total (8% and 1%, respectively).

166 The global distribution of PyC production also showed intricate regional patterns driven
 167 by variation in both the frequency at which fuel stocks were exposed to fire and the magnitude
 168 of the fuel stocks that were combusted during the fires that occurred (supplementary Figures
 169 S3 and S4). Fire frequency was ultimately the key determinant of PyC production rate and
 170 this explains why the tropics and subtropics were the dominant source regions. Although
 171 savannah fires affected low fuel stocks ($0.2\ kg\ C\ km^{-2}$ on average; supplementary information

172 text S2), these fires occurred frequently and were spatially extensive (supplementary Figure
173 S5 and table S2). They thus made the largest contribution to the global PyC production flux
174 ($125 \text{ Tg C year}^{-1}$ on average). Although tropical deforestation fires affected approximately 1%
175 of the area of savannah fires, they affected large stocks of fuel (8.7 kg C km^{-2} on average;
176 supplementary table S2) and were thus second largest driver of global PyC production,
177 contributing $49 \text{ Tg C year}^{-1}$. The area affected by non-deforestation tropical forest fires was
178 more than a factor of 4 larger than that of deforestation fires, however fuel consumption was
179 relatively low (2.3 kg C km^{-2} on average; supplementary table S2). These fires provide the
180 third major component of the global PyC production flux ($34 \text{ Tg C year}^{-1}$). Overall, 81% of
181 total global PyC production in the period 1997-2016 occurred in savannahs (49%) and
182 tropical forests (32%).

183



184
185

186 **Figure 4:** Annual average PyC production rates for the period 1997-2016 from GFED4s+PyC, based on central
187 production factors (see Figure 2). **(Left panel)** The global distribution of PyC production expressed in g C m^{-2}
188 year^{-1} . **(Right panel)** The total production of PyC (Tg C year^{-1}) in 15° latitudinal bands segregated according to
189 the fire type, including: savannah fires (SAVA); non-deforestation tropical forest fires (TROF); tropical
190 deforestation fires (DEFO); agricultural fires (AGRI); temperate forest fires (TEMF); extratropical grassland fires
191 (EXGR), and; boreal forest fires (BORF).

192
193

194 **Global Carbon Budget Implications**

195 Here we have quantified the global gross sink of atmospheric carbon caused by the
196 transfer of photosynthetically-sequestered biomass carbon to stocks of PyC during
197 vegetation fires. Our central global PyC production flux estimate (256 Tg C year⁻¹) is nontrivial
198 within the context of the global carbon cycle (Figure 1), equating to 12% of the global carbon
199 emissions flux due to biomass burning and around 8% of the land sink for atmospheric CO₂
200 (~3.0-3.2 Tg C year⁻¹)^{2,4}. This flux is in addition to the smaller global flux of 2 Tg C year⁻¹
201 caused by the emission of PyC in smoke from vegetation fires (according to estimates made
202 using GFED4s in the years 1997-2016)¹.

203 The magnitude of our global estimate for PyC production indicates that the
204 transformation of biomass carbon to PyC in vegetation fires has the potential to significantly
205 influence the atmospheric stock of carbon. A net sink of atmospheric carbon to stocks of PyC
206 can be expected to develop if the flux associated with its production is unmatched by re-
207 mineralisation fluxes from legacy PyC stocks in terrestrial and marine pools (Figure 1). Earth
208 System Models (ESMs) are the most sophisticated tools available to quantify the exchange
209 of carbon between the atmosphere and these pools in time periods for which robust empirical
210 data is sparse or unavailable. Despite foregoing attempts to highlight the importance of PyC
211 production for carbon storage over timescales relevant to anthropogenic climate change and
212 its mitigation^{36,37,47}, the absence of the PyC cycle from ESMs has restricted the scope for
213 quantifying its role in the carbon cycle¹⁵. The method introduced here allows for the routine
214 integration of PyC production into fire-enabled vegetation models in a manner that
215 systematically considers the spatial distribution of fire, the composition of the fuel stocks
216 affected and the specific PyC production factors that apply to individual fuel components.
217 This procedure would be relatively simple to implement in other fire-enabled vegetation
218 models used by ESMs, meaning that the major outstanding challenge to quantifying the net
219 exchange of carbon between the atmosphere and PyC stocks with ESMs will be to improve
220 constraints over its storage and residence time in terrestrial and marine pools (Figure 1)^{14,15}.

221 We also show that the PyC cycle must be integrated into ESMs if they are to accurately
222 represent the more general role of fire in the carbon cycle. At present, the fate of 11% of the
223 global biomass carbon stocks affected annually by fire is misrepresented in global models.
224 Recent estimates suggest that total carbon emissions from biomass burning in the period

225 1750-2015 amounted to around 500 Pg C (averaging 1.9 Pg C year⁻¹)⁴¹. Under the
226 assumption that the modern global PyC production flux maintained a constant ratio with the
227 carbon emissions flux throughout this period, we estimate that approximately 60 Pg C was
228 transferred to PyC stocks since the beginning of the industrial revolution. This value is
229 equivalent to 33-40% of the carbon lost from biomass pools due to land use change in the
230 same time period (145-180 Pg C)^{4,48}.

231 The production flux of PyC represents the quantity of carbon that models would
232 otherwise treat as unburned dead or living vegetation with a residence time in terrestrial pools
233 on the order of months to decades^{9,12,26,39,40,49}. This misrepresentation of the legacy effects
234 of fire thus introduces potentially significant errors to carbon accounting exercises. Moreover,
235 as PyC dynamics are not represented in the ESMs used to make global carbon budget
236 calculations, this pool may represent a missing sink or source of carbon to the
237 atmosphere^{15,50}. Our PyC production estimate is equivalent to 41% of the global carbon
238 budget imbalance caused by overestimated emissions and/or underestimated sinks in the
239 past decade (600 Tg C year⁻¹)², suggesting that errors resulting from the absence of PyC
240 from ESMs may contribute significantly to global carbon accounting uncertainties.

241 The production of PyC may also become an increasingly important process for global
242 carbon cycling in future centuries. Although global burned area has declined in at least the
243 past two decades due predominantly to the conversion of savannah and grassland to
244 agriculture^{51,52}, recent fire modelling studies generally agree that this decline is unlikely to
245 continue past the year 2050⁵³⁻⁵⁵. It is also likely that a higher fraction of global burned area
246 will be distributed in forests where significant stocks of vegetation carbon are held^{54,56,57}. As
247 woody fuels generate more PyC per unit of biomass carbon than other fuels (Figure 1), the
248 spread of fire into forests can be expected to disproportionately enhance global PyC
249 production (supplementary Figure S2). Although it is less clear how fire prevalence will
250 change in tropical and temperate forests owing to a stronger human control over burning in
251 these regions^{51,54}, recent increases in fire extent caused by increasing drought frequency in
252 Amazonia are already counteracting reductions in the extent of deforestation fires⁵⁸.
253 Notwithstanding the significant uncertainty that exists in model predictions of future fire
254 regimes, there are strong indications that PyC production rates will increase in some of the
255 Earth's most carbon-dense regions in response to a changing climate^{7,9,59}. This implies that

256 the buffer for atmospheric CO₂ emissions resulting from PyC production will grow in future
257 centuries.

258 **Methods**

259 ***Global Fuel Consumption Modelling in GFED4s***

260 In GFED4s, carbon emissions to the atmosphere are quantified based on burned area
261 and fuel consumption per unit burned area. Burned area is derived from satellite⁶⁰ and fires
262 that are too small to be detected by regular burned area algorithms are derived statistically
263 based on active fire detections and relations with vegetation indices⁶¹. Fuel consumption is
264 modelled using a satellite-driven biogeochemical model¹ and tuned to match observations⁶².
265 Most of the underlying satellite input datasets have a 500 × 500 m resolution but are
266 aggregated to the model resolution of 0.25° × 0.25°. Total fuel consumption is based on fuel
267 consumption of several fuel components including leaves, grasses, litter, fine woody debris,
268 coarse woody debris (CWD), and standing wood. For more information on the GFED4s
269 modelling approach, the reader is directed to reference¹.

270 To calculate PyC production within GFED4s we added a production factor, P_{PyC}, which
271 quantifies the production of PyC per unit carbon emitted (g PyC g⁻¹ C emitted). Until now, the
272 principle obstacle to performing a global modelling exercise of this type has been the lack of
273 a sufficiently rich and standardised dataset with which to constrain representative values for
274 P_{PyC}. The remainder of this section details how representative PyC production factors were
275 collated and summarised and subsequently integrated into the fuel consumption model of
276 GFED4s.

277 Our estimates of uncertainty in PyC production relate only to variability in PyC
278 production factors and do not include uncertainty in fuel consumption propagating from
279 GFED4s. Uncertainties in GFED4s fuel consumption are discussed in great detail in ref. ¹
280 and are predominantly the result of uncertainties in the satellite detection of small fires using
281 thermal anomalies and burn scars. Based on the level of agreement with regional-level
282 estimates it is estimated that the burned area data used in GFED have a 1 standard deviation
283 uncertainty range of 50% but are probably underestimated due to the difficulty in capturing
284 small fire burned area and the choice of a conservative approach in ref. ⁶¹. As carbon
285 emissions and PyC production are co-dependent on burned area, estimation errors relating

286 to fire detection introduce scalar uncertainties. Uncertainty in fuel consumption is a smaller
287 component of the overall uncertainty in GFED4s¹ emission estimates and has been reduced
288 from previous versions through its incorporation of a global dataset of fuel consumption
289 estimates⁶².

290 ***Collating a Global Dataset of PyC Production Factors***

291 We compiled a new database of P_{PYC} factors from a global collection of 21 published
292 studies which reported on PyC production in 91 burn units, as well as two new datasets
293 produced by the authors with 23 burn units reported for the first time here, and standardised
294 their reporting. All studies used one of the following two broad approaches to quantifying the
295 impacts of fire on the biomass carbon stocks, either: pre-fire and post-fire stocks of biomass
296 carbon and PyC are measured, or; space-for-time substitution is used to constrain burned
297 and unburned stocks of biomass carbon and PyC, which are assumed to be equivalent to
298 pre-fire and post-fire stocks, respectively. Hereafter, the terms “pre-fire” and “post-fire” are
299 used to refer to both types of assessment. Here we focus only on PyC present in charcoal
300 and ash on the ground following fire⁶³ as well as charred vegetation. PyC emitted with smoke,
301 transported in the atmosphere and deposited over a distant area is not included as this
302 process has been studied in separate dedicated studies conducted by atmospheric
303 scientists²⁴ and represents a relatively small flux in comparison (<5%)^{13,14}.

304 The P_{PYC} values were calculated for each of six classes of widely used biomass
305 components: coarse woody surface fuels (CWSF), including coarse woody debris or downed
306 wood defined by typical diameter thresholds of >7.6 cm or >10 cm^{64,65}; fine woody surface
307 fuels (FWSF), including fine woody debris or any other woody debris with diameters below
308 the thresholds for CWSF; coarse woody aboveground fuels (CWAGF), including trees or
309 branches with diameters greater than the thresholds for CWSF; fine woody aboveground
310 fuels (FWAGF), including material described as shrubs, trees or branches with diameters
311 below the thresholds for CWSF; non-woody surface fuels (NWSF), including litter, understory
312 vegetation, grass, root mat and any other form of non-woody material directly in contact with
313 the ground surface^{65,66}, and finally; non-woody aboveground fuels (NWAGF), including
314 foliage, leaves, needles, crown fuels and any other form of non-woody material that attaches
315 to standing wood structures above the ground surface.

316 For each biomass component, P_{PYC} was calculated using the following equation (1):

317

$$P_{PyC} = \frac{C_{Py}}{C_{PRE} - C_{POST}}$$

318

319

320

321

where C_{Py} is the mass of PyC created during the fire that was attributed to the component, C_{PRE} was the pre-fire stock of biomass carbon in the component, and C_{POST} was the post-fire stock of biomass carbon in the component. C_{Py} , C_{PRE} and C_{POST} were all expressed in the units g C km⁻².

322

323

324

325

326

327

328

329

330

331

332

333

334

Criteria were applied as filters to the dataset in order to ensure that P_{PyC} could be calculated in a consistent and representative manner. Specifically, P_{PyC} was calculated if the following conditions were met: first, both pre-fire and post-fire biomass stocks were reported and carbon content (%) was either measured or assumed based on representative values from the literature; second, post-fire stocks of pyrogenic organic matter (charcoal, ash and charred vegetation) were reported and their PyC content (%) was either measured or assumed based on representative values from the literature; third, the type of fire that occurred was representative of a widespread regional fire type (e.g. wildfires, slash-and-burn deforestation, and prescribed fire); fourth, in experimental fires, the biomass carbon stock was designed to replicate the density and structure of biomass carbon stocks observed in the field and the burning efficiency was not optimised or adapted as a factor of the study design; fifth, the post-fire sampling exercise was completed within 3 months of the fire such that losses of PyC through erosion and mineralisation were minimised.

335

336

337

338

339

340

341

342

343

344

345

346

Like biomass carbon, total PyC stocks are distributed across several components including charcoal and ash on the ground, charcoal attached to coarse woody debris, and charcoal attached to aboveground vegetation¹³. The majority of the studies included in the production factor dataset matched the studied PyC components to individual biomass carbon components from which they were known to derive. However, as some individual components of PyC stocks can have a mixture of sources that are indistinguishable from their location or appearance alone, it was occasionally necessary to make assumptions about the biomass components that were sources of these components. This was done on a study-by-study basis. In cases where the source of each PyC component was not explicitly stated, the following procedural steps were adhered to. On a first basis, the PyC component was assigned to a biomass component according to the most probable source inferred, but not explicitly stated, in the primary literature. Second, where more than one biomass component

347 was inferred to be a source of the PyC stock in the primary literature, the PyC stock was
348 weighted proportionally to the pre-fire stock of carbon present in each of the implicated
349 biomass components. Otherwise, if no sources of PyC were inferred in the primary literature
350 it was necessary to make independent assumptions about the source of PyC in a manner
351 that was consistent with the other studies included in the dataset and our collective
352 experience of quantifying PyC production in the field.

353 ***Summarising Production Factor Values for use in GFED4s+PyC***

354 Our global database suggested that coarse woody surface fuels (CWSF) and
355 aboveground fuels (CWAGF) produce significantly more PyC, relative to carbon emitted, than
356 other fuel classes (P_{PyC} averaged 0.25 and 0.31 g PyC g⁻¹ C emitted, respectively; Figure 2).
357 In contrast, the mean P_{PyC} values for fine woody surface fuels (FWSF) and fine woody
358 aboveground fuels (FWAGF; 0.12 and 0.076 g PyC g⁻¹ C emitted, respectively) did not differ
359 significantly from those of non-woody surface fuels (NWSF) or non-woody aboveground fuels
360 (NWAGF; 0.099 and 0.062 g PyC g⁻¹ C emitted, respectively). These results are consistent
361 with previous studies, which suggest that large-diameter woody fuels burn less completely
362 and produce PyC in greater proportions than finer fuels^{23,36,67}.

363 For each class, the mean PyC production factor was used as the central estimate for
364 P_{PyC} , while the confidence interval around the mean P_{PyC} was calculated through a
365 bootstrapping procedure. Specifically, the available PyC production factors from the dataset
366 were resampled 50,000 times, the mean P_{PyC} was calculated for each resample, and the
367 95% confidence interval was calculated as the middle 95% of the observed 50,000 means
368 (i.e. those ranked 1,250th to 48,750th).

369 According to analysis of variance (ANOVA) with a Tukey Honest Significant Difference
370 post-hoc test, no significant differences in mean P_{PyC} were observed between the
371 distributions of P_{PyC} for coarse, fine, and non-woody fuels positioned at the ground surface
372 and those same fuels located above the ground surface. Therefore, the P_{PyC} values applied
373 in GFED4s+PyC were based on the distribution of values in three simplified fuel classes
374 (Figure 2): coarse woody fuels (CWF: mean 0.26 g PyC g⁻¹ C; 95% confidence interval 0.18-
375 0.39 g PyC g⁻¹ C), fine woody fuels (FWF: mean 0.096 g PyC g⁻¹ C; 95% confidence interval
376 0.064-0.15 g PyC g⁻¹ C) and non-woody fuels (NWF: mean 0.091 g PyC g⁻¹ C; 95%
377 confidence interval 0.074-0.11 g PyC g⁻¹ C).

378 ***Assigning PyC Production Factors in GFED4s+PyC***

379 P_{PYC} values were assigned to each of the native fuel classes of GFED4s¹, which are:
380 leaves; grasses; surface fuels (including litter and fine woody debris); coarse woody debris
381 (CWD), and; standing wood (including trunks, stems and branches). Mean P_{PYC} values and
382 bootstrapped confidence interval values for CWF, FWF and NWF from the global dataset
383 were used to define representative P_{PYC} values for each of the GFED4s fuel classes (Figure
384 2). Full details regarding the assignment of P_{PYC} values to each GFED4s fuel class are
385 provided in the supplementary information (text S3 and table S3). Briefly: leaf, litter, grass
386 were assigned the relevant P_{PYC} values of NWF; fine woody debris and coarse woody debris
387 were assigned the values of FWF and CWF, respectively, and; P_{PYC} values for standing wood
388 were applied in a spatially explicit manner as weighted combinations of the P_{PYC} values for
389 CWF (for carbon in trunks) and FWF (for carbon in branches). The weighted CWF:FWF ratio
390 was assigned according to empirical relationships defining biomass carbon apportionment to
391 branches and trunks in the various forest types of the GFED4s land cover scheme
392 (supplementary information text S3 and table S4)⁶⁸.

393 ***Quantifying ENSO Impacts on PyC Production***

394 To investigate the influence of pan-tropical climatic variability driven by the El Niño
395 Southern Oscillation on the production of PyC, we replicated the analysis presented by Chen
396 et al. (ref. ⁴⁶) with a focus on PyC production rather than carbon emissions. The pan-tropics
397 were defined as consisting of Central America (CEAM); Northern Hemisphere South America
398 (NHSA); Southern Hemisphere South America (SHSA); Northern Hemisphere Africa (NHAF);
399 Southern Hemisphere Africa (SHAF); Southeast Asia (SEAS); Equatorial Asia (EQAS), and;
400 Australia (AUST; supplementary Figure S6). PyC production in El Niño and La Niña phases
401 was compared for the major fire season periods defined in each tropical region by Chen et
402 al. (ref. ⁴⁶); the reader is referred to their study for a thorough explanation of the rationale for
403 selecting these comparison periods. We summed PyC production in the major fire season
404 period of each region and disaggregated this total to forest and non-forest fires according to
405 the dominant land cover type in the GFED4s land cover scheme (based on the MODIS Land
406 Cover Type Climate Modelling Grid product MCD12C1)⁶⁹.

407 **Apportioning Sources of PyC**

408 Following GFED4s+PyC model runs, PyC production was assigned to specific sources
409 following a method developed previously for use in GFED4s model runs^{1,70}. Specifically, PyC
410 production occurring as a result of non-deforestation fires was disaggregated in each cell to
411 tropical forest, savannah/grassland, boreal forest, temperate forest, and agricultural fires
412 using an existing algorithm that utilises fractional tree cover, climate and fire persistence
413 variables. The reader is referred to ref. ⁷⁰ for a full discussion of this algorithm. We added an
414 additional latitudinal constraint (30 °N-30 °S) to further disaggregate the savannah
415 compartment, which thus separates tropical savannahs and grasslands from extratropical
416 grasslands.

417 **References**

- 418 1. van der Werf, G. R. *et al.* Global fire emissions estimates during 1997–2016. *Earth*
419 *Syst. Sci. Data* **9**, 697–720 (2017).
- 420 2. Le Quéré, C. *et al.* Global Carbon Budget 2018. *Earth Syst. Sci. Data* **10**, 2141–2194
421 (2018).
- 422 3. Houghton, R. A. & Nassikas, A. A. Global and regional fluxes of carbon from land use
423 and land cover change 1850-2015. *Global Biogeochem. Cycles* **31**, 456–472 (2017).
- 424 4. Ciais, P. *et al.* in *Climate Change 2013: The Physical Science Basis. Contribution of*
425 *Working Group I to the Fifth Assessment Report of the Intergovernmental Panel on*
426 *Climate Change* (eds. Stocker, T. F. *et al.*) 465–570 (Cambridge University Press,
427 2013).
- 428 5. Crutzen, P. J. & Andreae, M. O. Biomass Burning in the Tropics: Impact on
429 Atmospheric Chemistry and Biogeochemical Cycles. *Science* **250**, 1669–1678 (1990).
- 430 6. Ballantyne, A. P., Alden, C. B., Miller, J. B., Tans, P. P. & White, J. W. C. Increase in
431 observed net carbon dioxide uptake by land and oceans during the past 50 years.
432 *Nature* **488**, 70–72 (2012).
- 433 7. Bowman, D. *et al.* Fire in the Earth system. *Science* **324**, 481–4 (2009).
- 434 8. Pan, Y. *et al.* A Large and Persistent Carbon Sink in the World's Forests. *Science* **333**,
435 988–993 (2011).
- 436 9. Hantson, S. *et al.* The status and challenge of global fire modelling. *Biogeosciences*
437 **13**, 3359–3375 (2016).
- 438 10. Rabin, S. S. *et al.* The Fire Modeling Intercomparison Project (FireMIP), phase 1:
439 Experimental and analytical protocols with detailed model descriptions. *Geosci. Model*
440 *Dev.* **10**, 1175–1197 (2017).
- 441 11. Kuhlbusch, T. A. J. Black Carbon and the Carbon Cycle. *Science* **280**, 1903–1904
442 (1998).
- 443 12. Lehmann, J. *et al.* Australian climate–carbon cycle feedback reduced by soil black
444 carbon. *Nat. Geosci.* **1**, 832–835 (2008).
- 445 13. Santín, C. *et al.* Towards a global assessment of pyrogenic carbon from vegetation
446 fires. *Glob. Chang. Biol.* **22**, 76–91 (2016).

- 447 14. Bird, M. I., Wynn, J. G., Saiz, G., Wurster, C. M. & McBeath, A. The Pyrogenic Carbon
448 Cycle. *Annu. Rev. Earth Planet. Sci.* **43**, 273–298 (2015).
- 449 15. Landry, J.-S. & Matthews, H. D. The global pyrogenic carbon cycle and its impact on
450 the level of atmospheric CO₂ over past and future centuries. *Glob. Chang. Biol.* **23**,
451 3205–3218 (2017).
- 452 16. Schmidt, M. W. I. Carbon budget in the black. *Nature* **427**, 305–307 (2004).
- 453 17. Reisser, M., Purves, R. S., Schmidt, M. W. I. & Abiven, S. Pyrogenic Carbon in Soils:
454 A Literature-Based Inventory and a Global Estimation of Its Content in Soil Organic
455 Carbon and Stocks. *Front. Earth Sci.* **4**, 1–14 (2016).
- 456 18. Ohlson, M., Dahlberg, B., Økland, T., Brown, K. J. & Halvorsen, R. The charcoal carbon
457 pool in boreal forest soils. *Nat. Geosci.* **2**, 692–695 (2009).
- 458 19. Koele, N. *et al.* Amazon Basin forest pyrogenic carbon stocks: First estimate of deep
459 storage. *Geoderma* **306**, 237–243 (2017).
- 460 20. Masiello, C. A. & Druffel, E. R. M. Black Carbon in Deep-Sea Sediments. *Science* **280**,
461 1911–1913 (1998).
- 462 21. Schmidt, M. W. I. & Noack, A. G. Black carbon in soils and sediments: Analysis,
463 distribution, implications, and current challenges. *Global Biogeochem. Cycles* **14**, 777–
464 793 (2000).
- 465 22. Dittmar, T. & Paeng, J. A heat-induced molecular signature in marine dissolved organic
466 matter. *Nat. Geosci.* **2**, 175–179 (2009).
- 467 23. Wagner, S., Jaffé, R. & Stubbins, A. Dissolved black carbon in aquatic ecosystems.
468 *Limnol. Oceanogr. Lett.* **3**, 168–185 (2018).
- 469 24. Bond, T. C. *et al.* Bounding the role of black carbon in the climate system: A scientific
470 assessment. *J. Geophys. Res. Atmos.* **118**, 5380–5552 (2013).
- 471 25. Booth, B. & Bellouin, N. Black carbon and atmospheric feedbacks. *Nature* **519**, 167–
472 168 (2015).
- 473 26. Kuzyakov, Y., Bogomolova, I. & Glaser, B. Biochar stability in soil: Decomposition
474 during eight years and transformation as assessed by compound-specific¹⁴C analysis.
475 *Soil Biol. Biochem.* **70**, 229–236 (2014).
- 476 27. Schneider, M. P. W., Hilf, M., Vogt, U. F. & Schmidt, M. W. I. The benzene
477 polycarboxylic acid (BPCA) pattern of wood pyrolyzed between 200°C and 1000°C.
478 *Org. Geochem.* **41**, 1082–1088 (2010).
- 479 28. Wiedemeier, D. B. *et al.* Aromaticity and degree of aromatic condensation of char. *Org.*
480 *Geochem.* **78**, 135–143 (2015).
- 481 29. Jaffé, R. *et al.* Global charcoal mobilization from soils via dissolution and riverine
482 transport to the oceans. *Science* **340**, 345–7 (2013).
- 483 30. Coppola, A. I. *et al.* Global-scale evidence for the refractory nature of riverine black
484 carbon. *Nat. Geosci.* **11**, 584–588 (2018).
- 485 31. Coppola, A. I., Ziolkowski, L. A., Masiello, C. A. & Druffel, E. R. M. Aged black carbon
486 in marine sediments and sinking particles. *Geophys. Res. Lett.* **41**, 2427–2433 (2014).
- 487 32. Singh, B. P., Cowie, A. L. & Smernik, R. J. Biochar Carbon Stability in a Clayey Soil As
488 a Function of Feedstock and Pyrolysis Temperature. *Environ. Sci. Technol.* **46**, 11770–
489 11778 (2012).
- 490 33. Ziolkowski, L. A. & Druffel, E. R. M. Aged black carbon identified in marine dissolved
491 organic carbon. *Geophys. Res. Lett.* **37**, 4–7 (2010).
- 492 34. Preston, C. M. & Schmidt, M. W. I. Black (pyrogenic) carbon: a synthesis of current
493 knowledge and uncertainties with special consideration of boreal regions.
494 *Biogeosciences* **3**, 397–420 (2006).

- 495 35. Goldberg, E. D. *Black carbon in the environment: properties and distribution*. (John
496 Wiley and Sons, 1985).
- 497 36. Kuhlbusch, T. a. J. & Crutzen, P. J. Toward a global estimate of black carbon in
498 residues of vegetation fires representing a sink of atmospheric CO₂ and a source of
499 O₂. *Global Biogeochem. Cycles* **9**, 491–501 (1995).
- 500 37. Santín, C., Doerr, S. H., Preston, C. M. & González-Rodríguez, G. Pyrogenic organic
501 matter production from wildfires: a missing sink in the global carbon cycle. *Glob. Chang.
502 Biol.* **21**, 1621–1633 (2015).
- 503 38. Singh, N., Abiven, S., Torn, M. S. & Schmidt, M. W. I. Fire-derived organic carbon in
504 soil turns over on a centennial scale. *Biogeosciences* **9**, 2847–2857 (2012).
- 505 39. Schmidt, M. W. I. *et al.* Persistence of soil organic matter as an ecosystem property.
506 *Nature* **478**, 49–56 (2011).
- 507 40. Thurner, M. *et al.* Evaluation of climate-related carbon turnover processes in global
508 vegetation models for boreal and temperate forests. *Glob. Chang. Biol.* **23**, 3076–3091
509 (2017).
- 510 41. Van Marle, M. J. E. *et al.* Historic global biomass burning emissions for CMIP6
511 (BB4CMIP) based on merging satellite observations with proxies and fire models
512 (1750–2015). *Geosci. Model Dev.* **10**, 3329–3357 (2017).
- 513 42. Yang, J. *et al.* Century-scale patterns and trends of global pyrogenic carbon emissions
514 and fire influences on terrestrial carbon balance. *Global Biogeochem. Cycles* **29**, 1549–
515 1566 (2015).
- 516 43. Schultz, M. G. *et al.* Global wildland fire emissions from 1960 to 2000. *Global
517 Biogeochem. Cycles* **22**, 1–17 (2008).
- 518 44. Yang, J. *et al.* Spatial and temporal patterns of global burned area in response to
519 anthropogenic and environmental factors: Reconstructing global fire history for the 20th
520 and early 21st centuries. *J. Geophys. Res. Biogeosciences* **119**, 249–263 (2014).
- 521 45. Chen, Y., Morton, D. C., Andela, N., Giglio, L. & Randerson, J. T. How much global
522 burned area can be forecast on seasonal time scales using sea surface temperatures?
523 *Environ. Res. Lett.* **11**, (2016).
- 524 46. Chen, Y. *et al.* A pan-tropical cascade of fire driven by El Niño/Southern Oscillation.
525 *Nat. Clim. Chang.* **7**, 906–911 (2017).
- 526 47. Woolf, D., Amonette, J. E., Street-Perrott, F. A., Lehmann, J. & Joseph, S. Sustainable
527 biochar to mitigate global climate change. *Nat. Commun.* **1**, 1–9 (2010).
- 528 48. Houghton, R. A. & Nassikas, A. A. Global and regional fluxes of carbon from land use
529 and land cover change 1850–2015. *Global Biogeochem. Cycles* **31**, 456–472 (2017).
- 530 49. Surawski, N. C., Sullivan, A. L., Roxburgh, S. H., Meyer, C. P. M. & Polglase, P. J.
531 Incorrect interpretation of carbon mass balance biases global vegetation fire emission
532 estimates. *Nat. Commun.* **7**, 1–5 (2016).
- 533 50. Santín, C., Doerr, S. H., Preston, C. M. & González-Rodríguez, G. Pyrogenic organic
534 matter produced during wildfires can act as a carbon sink – a reply to Billings &
535 Schlesinger (2015). *Glob. Chang. Biol.* **24**, e399 (2018).
- 536 51. Andela, N. *et al.* A human-driven decline in global burned area. *Science* **356**, 1356–
537 1362 (2017).
- 538 52. Arora, V. K. & Melton, J. R. Reduction in global area burned and wildfire emissions
539 since 1930s enhances carbon uptake by land. *Nat. Commun.* (2018).
540 doi:10.1038/s41467-018-03838-0
- 541 53. Pechony, O. & Shindell, D. T. Driving forces of global wildfires over the past millennium
542 and the forthcoming century. *Proc. Natl. Acad. Sci.* **107**, 19167–19170 (2010).

Submitted manuscript draft of version of: Jones, M.W., Santín, C., van der Werf, G.R., **Doerr, S.H.** (2019) Global fire emissions buffered by the production of recalcitrant pyrogenic carbon. *Nature Geoscience* (published on 5th Aug. 2019, available at: <https://doi.org/10.1038/s41561-019-0403-x>). Note that the published version will be an updated version from this submitted draft.

- 543 54. Knorr, W., Arneth, A. & Jiang, L. Demographic controls of future global fire risk. *Nat.*
544 *Clim. Chang.* **6**, 781–785 (2016).
- 545 55. Flannigan, M. *et al.* Global wildland fire season severity in the 21st century. *For. Ecol.*
546 *Manage.* **294**, 54–61 (2013).
- 547 56. Flannigan, M. D. *et al.* Fuel moisture sensitivity to temperature and precipitation:
548 climate change implications. *Clim. Change* **134**, 59–71 (2016).
- 549 57. Wang, X. *et al.* Projected changes in daily fire spread across Canada over the next
550 century. *Environ. Res. Lett.* **12**, (2017).
- 551 58. Aragão, L. E. O. C. *et al.* 21st Century drought-related fires counteract the decline of
552 Amazon deforestation carbon emissions. *Nat. Commun.* **9**, 536 (2018).
- 553 59. Krawchuk, M. A. & Moritz, M. A. Burning issues: statistical analyses of global fire data
554 to inform assessments of environmental change. *Environmetrics* **25**, 472–481 (2014).
- 555 60. Giglio, L., Randerson, J. T. & van der Werf, G. R. Analysis of daily, monthly, and annual
556 burned area using the fourth-generation global fire emissions database (GFED4). *J.*
557 *Geophys. Res. Biogeosciences* **118**, 317–328 (2013).
- 558 61. Randerson, J. T., Chen, Y., Van Der Werf, G. R., Rogers, B. M. & Morton, D. C. Global
559 burned area and biomass burning emissions from small fires. *J. Geophys. Res.*
560 *Biogeosciences* **117**, (2012).
- 561 62. van Leeuwen, T. T. *et al.* Biomass burning fuel consumption rates: a field measurement
562 database. *Biogeosciences Discuss.* **11**, 8115–8180 (2014).
- 563 63. Bodí, M. B. *et al.* Wildland fire ash: Production, composition and eco-hydro-geomorphic
564 effects. *Earth-Science Rev.* **130**, 103–127 (2014).
- 565 64. Hyde, J. C., Smith, A. M. S., Ottmar, R. D., Alvarado, E. C. & Morgan, P. The
566 combustion of sound and rotten coarse woody debris: a review. *Int. J. Wildl. Fire* **20**,
567 163 (2011).
- 568 65. Lutes, D. C., Keane, R. E. & Caratti, J. F. A surface fuel classification for estimating fire
569 effects. *Int. J. Wildl. Fire* **18**, 802 (2009).
- 570 66. Sandberg, D. V., Ottmar, R. D. & Cushon, G. H. Characterizing fuels in the 21st
571 Century. *Int. J. Wildl. Fire* **10**, 381 (2001).
- 572 67. Knicker, H., Hilscher, A., González-Vila, F. J. & Almendros, G. A new conceptual model
573 for the structural properties of char produced during vegetation fires. *Org. Geochem.*
574 **39**, 935–939 (2008).
- 575 68. Thurner, M. *et al.* Carbon stock and density of northern boreal and temperate forests.
576 *Glob. Ecol. Biogeogr.* **23**, 297–310 (2014).
- 577 69. Friedl, M., Sulla-Menashe, D. MCD12C1 MODIS/Terra+Aqua Land Cover Type Yearly
578 L3 Global 0.05Deg CMG V006. (2015). doi:10.5067/MODIS/MCD12C1.006
- 579 70. van der Werf, G. R. *et al.* Global fire emissions and the contribution of deforestation,
580 savanna, forest, agricultural, and peat fires (1997–2009). *Atmos. Chem. Phys.* **10**,
581 11707–11735 (2010).
- 582 71. van der Werf, G. R. *et al.* Interannual variability in global biomass burning emissions
583 from 1997 to 2004. *Atmos. Chem. Phys.* 3423–3441 (2006).
- 584

585 **Supplementary Information** is linked to the online version of the paper at
586 www.nature.com/nature.

588 **Acknowledgements**

589 This work was funded by the Leverhulme Trust Grant awarded to SD (RPG-2014-095);
590 a Swansea University College of Science Fund awarded to MJ; a Vici grant awarded to GW
591 by the Netherlands organisation for scientific research (NWO), and a European Union
592 Horizon 2020 research and innovation grant awarded to CS (Marie Skłodowska-Curie grant
593 663830). We thank Cristina Aponte, Claudia Boot, Gareth Clay, Garry Cook, Francesca
594 Cotrufo, Philip Fearnside, Brett Goforth, Robert Graham, Michelle Haddix, Peter Homann,
595 Dale Hurst and Meaghan Jenkins for their assistance during the collation of the global dataset
596 of PyC production factors. We also thank Dr. Bill de Groot for his part in securing funding of
597 the Leverhulme Trust Grant.

598 **Author Contributions**

599 MJ, CS and SD designed the study. SD led the Leverhulme Trust grant funding the
600 majority of the work. MJ collated the PyC production factor dataset with support from CS. CS
601 and SD provided unpublished PyC production data. GW provided access to the GFED4s
602 code. MJ adapted the GFED4s code to include PyC production with the support of GW. MJ
603 conducted the formal analysis of production factor dataset and model outputs. All authors
604 contributed to the interpretation of the results. MJ wrote the manuscript text and produced all
605 figures. All authors contributed to the refinement of the manuscript text.

606 **Author Information**

607 Reprints and permissions information is available at www.nature.com/reprints. The
608 authors declare no competing interests. Correspondence and requests for materials should
609 be addressed to matthew.w.jones@swansea.ac.uk. The global dataset of PyC production
610 factors is available as supplementary data file (GlobalPyC_supplementarydataset.xls) and
611 will also be made publicly available through submission to the Pangaea Data Publisher for
612 Earth & Environmental Science. Supplementary information text S4 contains full reference to
613 the studies included in the production factor dataset.